# Neural representation of a high-dimensional perceptual space in macaque visual cortex

Jonathan D. Victor, Jonathan Witztum, Daniel J. Thengone, Eyal I. Nitzany, and Yunguo Yu

Division of Systems Neurology and Neuroscience, Brain and Mind Research Institute, Weill Cornell Medical College, New York, NY

## Introduction and Motivation

Perceptual spaces play a key role in intermediate visual processing, as they constitute representations that support discrimination, categorization, working memory, and other judgments. The classical perceptual space of color has three dimensions, but others, such as faces and textures, have very high dimension. Representing such spaces within biological constraints is challenging. To probe how visual cortex does this, we studied responses of macaque single neurons to a well-characterized 10-dimensional perceptual domain.

This model domain consists of black-and-white textures. Its 10 parameters are image statistics describing black/white balance and nearest-neighbor correlations (Victor and Conte 2012). The space is a useful model because it captures the informative local image statistics of natural scenes (Tkačik et al., 2010). Human perceptual sensitivities are optimally deployed within this space to match the informativeness of the space's axes (Hermundstad et al., 2014).

Perceptual studies suggest that this space is represented in two ways: in an opponent fashion, leading to an approximately Euclidean perceptual metric for threshold tasks (Conte et al., VSS 2015), and in a distributed one, leading to a highly curved metric for suprathreshold judgments (Rizvi et al., VSS 2014). Here we sought to identify the neural basis of these representations, via single-unit recordings in macaque visual cortex.

## Methods

#### Physiological methods

Macaque V1 and V2

Anesthesia: sufentanil and propofol Neuromuscular blockade: rocuronium

#### Recordings

53.4013 VSS2015

> 6-tetrode array, each tetrode independently movable Spike sorting, on- and off-line (KlustaKwik and Klusters) Lesions at each tetrode following all recordings

#### Stimuli

16 x 16 patches of textures

Check size and orientation optimized for "target" unit Stimuli presented in randomized order

#### Axis experiments (9 macaques):

41 stimuli: two positive and two negative values per axis, and the origin of the space

64 examples of each stimulus

Regression of first principal component of smoothed firing rate vs. each image statistic value

Significance determined by shuffle test

283 neurons histologically localized in V1 (87 sites)

184 neurons histologically localized in V2 (46 sites)

#### Planes experiments (2 macaques):

49 stimuli: six values on each of 8 directions in plane, and the origin of the space

Planes determined according to target unit(s)

Preliminary data from selected neurons at 44 sites in V1 and V2

## Stimulus parameters: the 10 axes

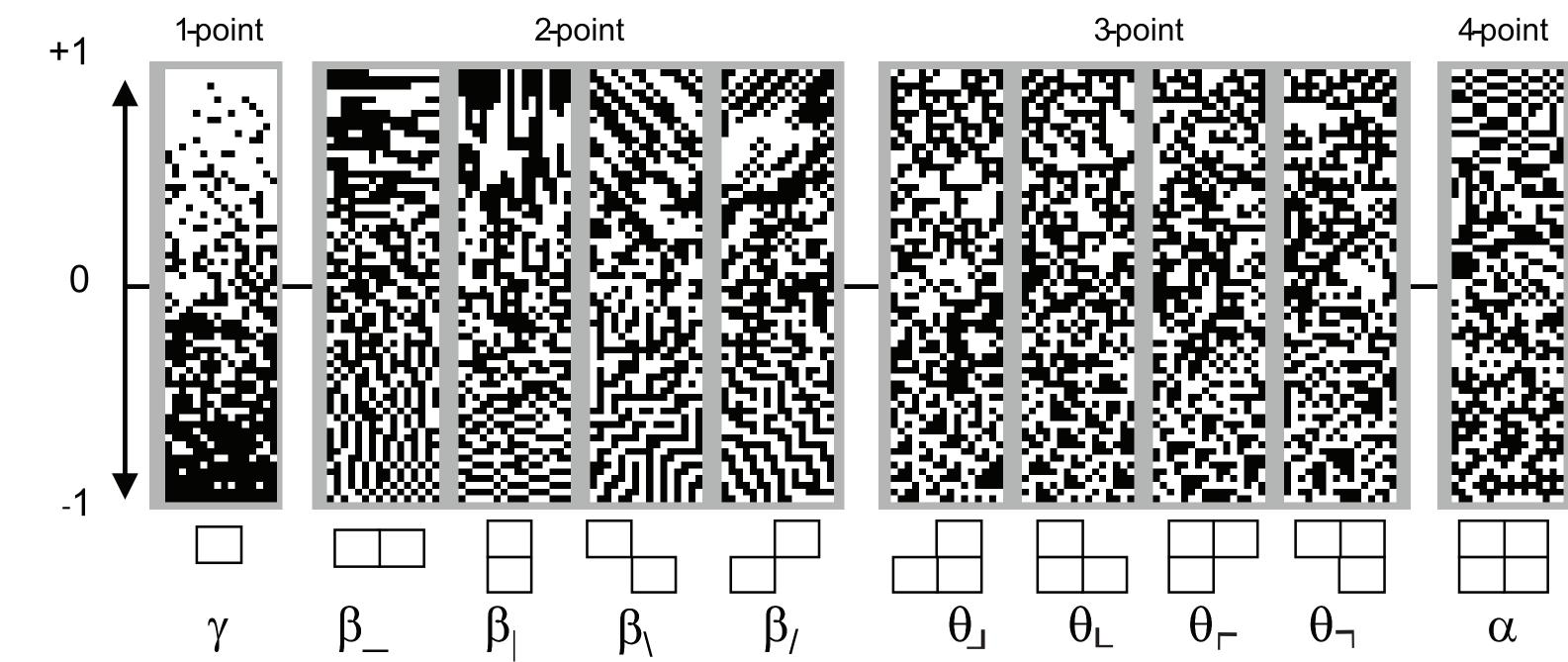
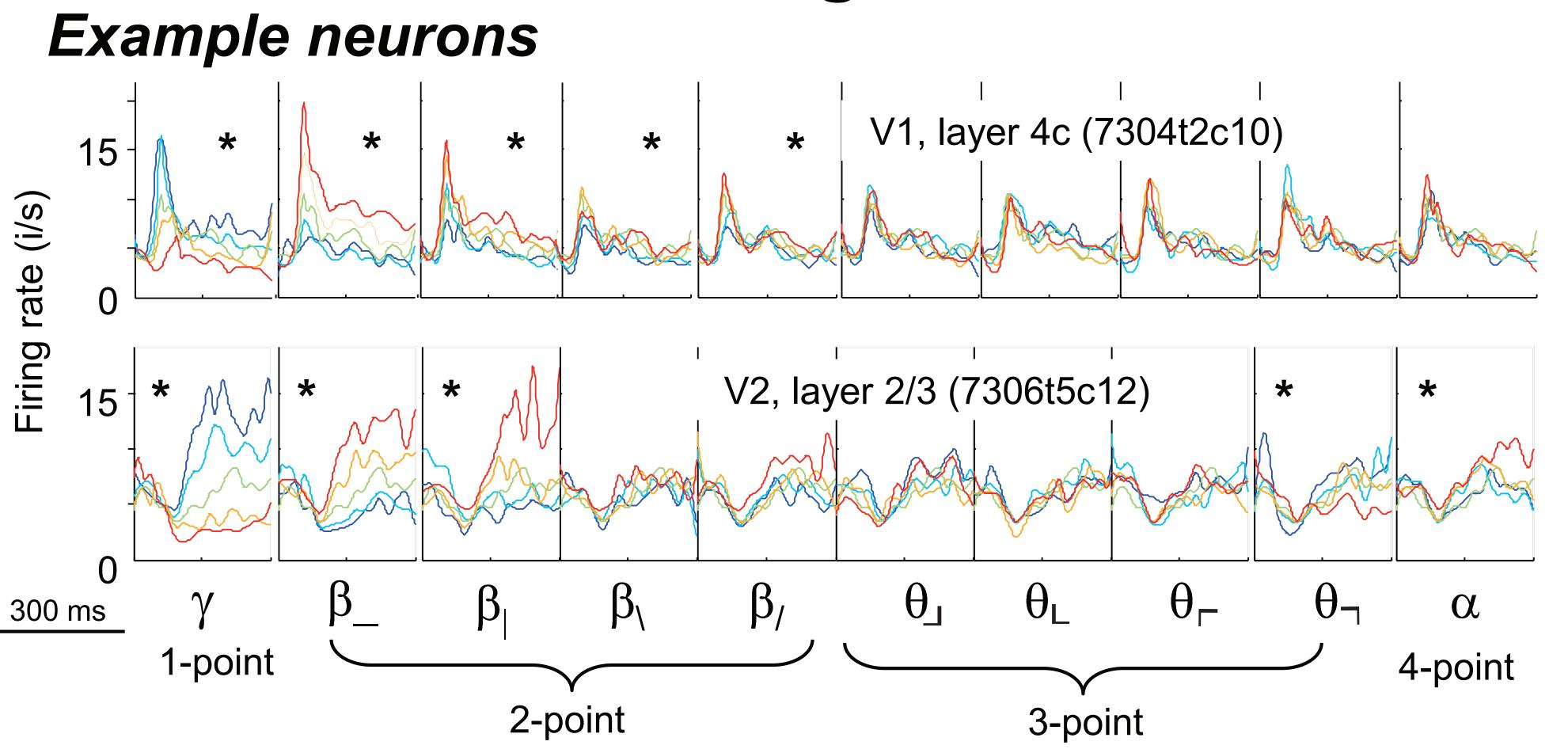


Image statistic values range from -1 to 1; 0 indicates random.  $\gamma$  is the difference in the fraction of bright vs. dark checks. The four  $\beta$  's are 2-point correlations, in the two cardinal and two diagonal directions. The four  $\theta$  's are 3-point correlations.  $\alpha$  is a 4-point correlation.

## Results: along the 10 axes

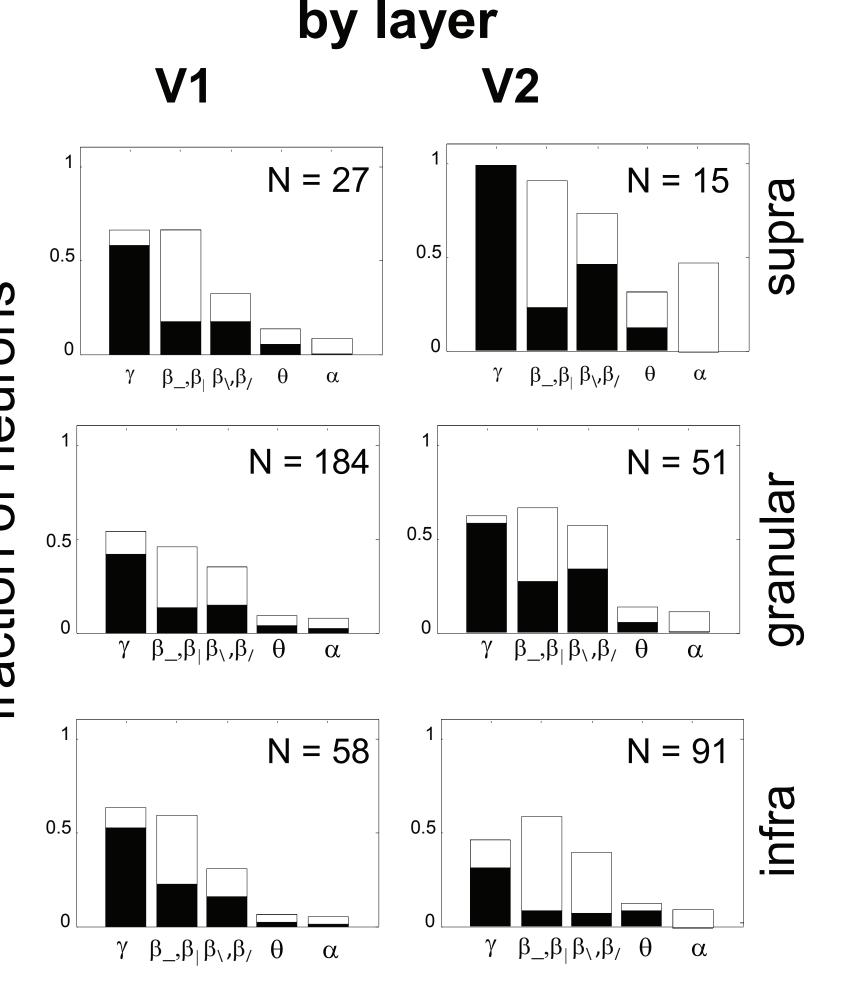


Smoothed firing rates of responses to stimuli along the coordinate axes. The V1 input-layer neuron is modulated by all 1- and 2-point statistics but not by 3- and 4-point statistics. The V2 supragranular neuron is modulated by image statistics of all orders.

Image statistic values are indicated by color: 0.4 (red) to -0.4 (blue) for the 1-point statistic  $\gamma$ , 0.8 to -0.8 for 2-, 3- and 4- point statistics  $\beta$ ,  $\theta$ , and  $\alpha$ . \* denotes significant (p<0.05) dependence.

# Population summary overall V1 V2 N = 184 regression coefficient: > 0 $\sqrt{N}$ raction of neurons with a significant occurrence on each image ratistic. For 3-point and 4-point statistics

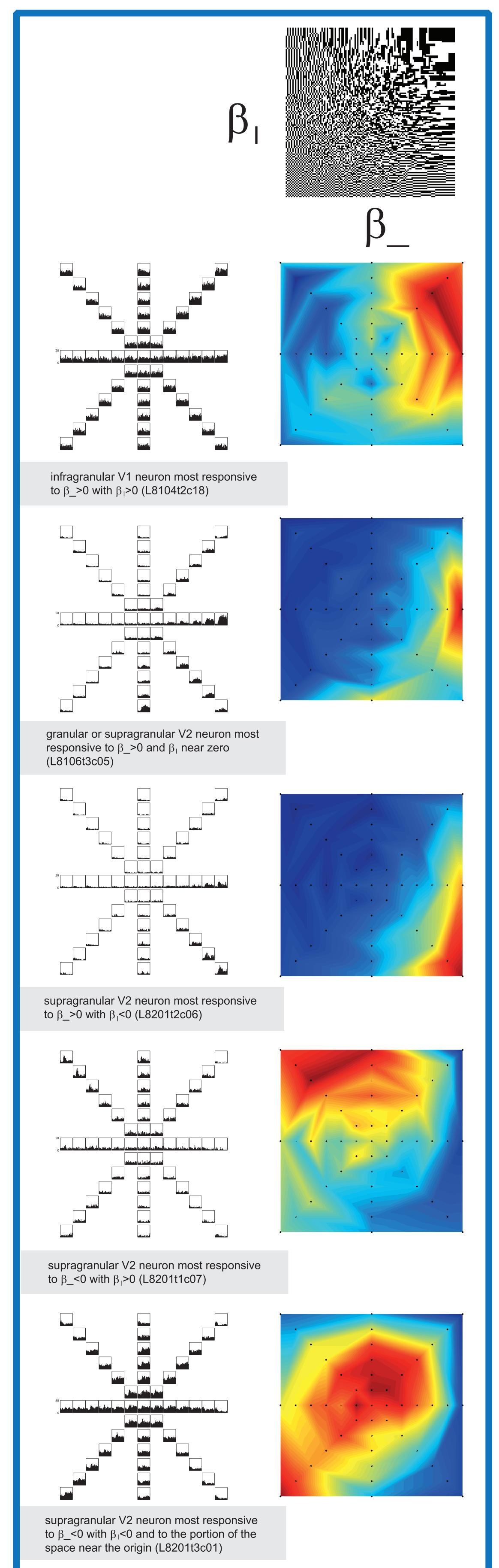
Fraction of neurons with a significant (p<0.05) dependence on each image statistic. For 3-point and 4-point statistics ( $\theta$  and  $\alpha$ ), this fraction is twice as high in V2 as in V1. The bias towards negative regression coefficients for  $\gamma$  indicates a preference for darks in V1 and V2.

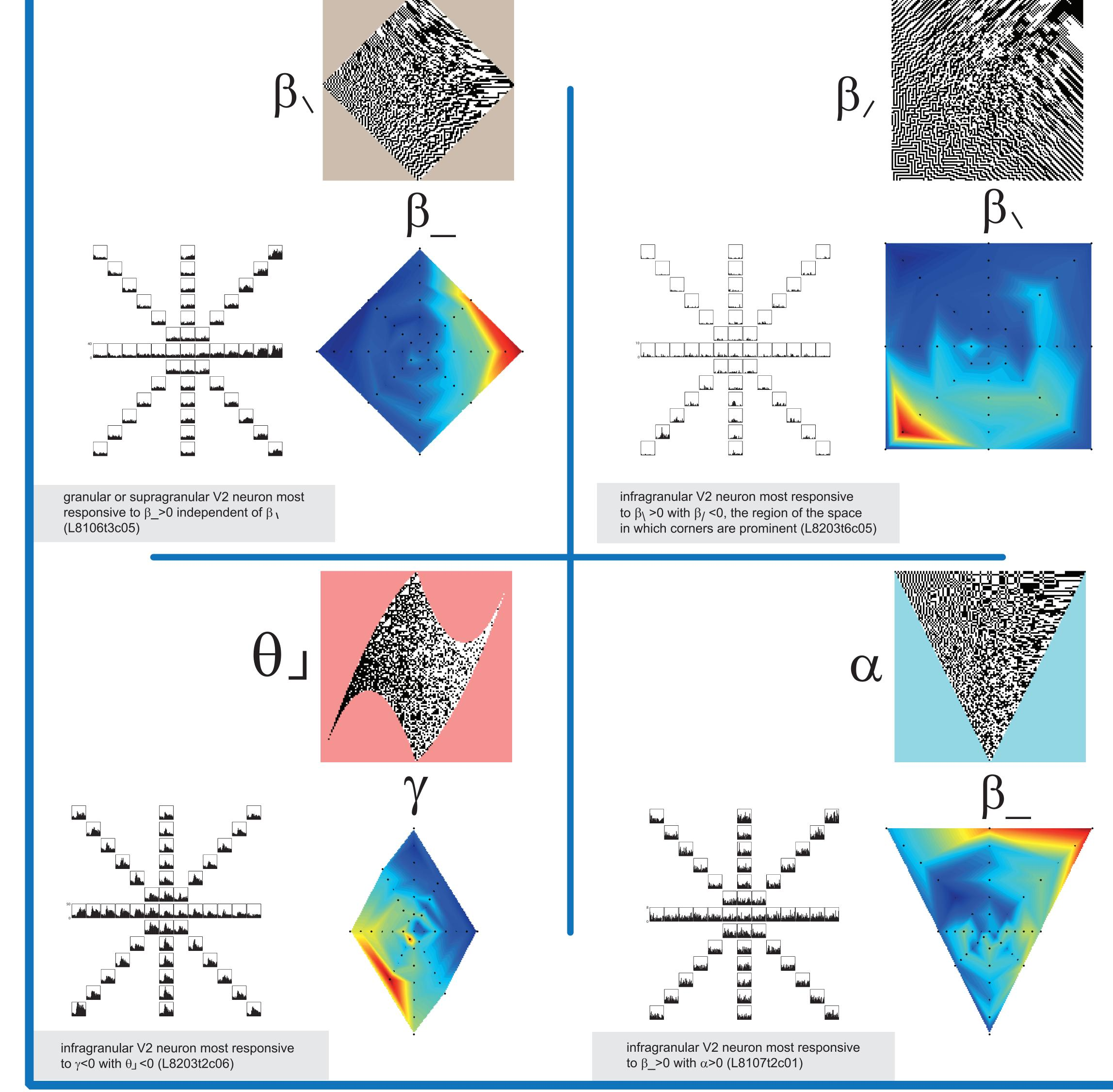


infragranular V1 neuron most responsive to  $\gamma$ <0 with  $\beta$ \_>0 (L8104t2c12) granular or supragranular V2 neuron most granular or supragranular V2 neuron mos responsive to  $\gamma$ <0 with  $\beta$  >0 (L8202t2c08) القرير المطارع granular V2 neuron most responsive to  $\gamma$ >0 with  $\beta$  <0 (L8203t2c06)

Panels show PSTH's of neural responses to pairwise combinations of image statistics, i.e., a plane of the stimulus domain. We measured responses to stimuli positioned at 6 points along each of 8 rays (PSTH's plotted along the spokes), and to the random texture (PSTH plotted at the center). Heat maps show the mean firing rate; the points indicate the locations in the plane that were sampled, and color scale is normalized to the maximal firing rate for each neuron. Typical neurons responded selectively to specific combinations of image statistics.

# Results: in coordinate planes





## Summary and Conclusions

## Individual image statistics (the axes):

- Neurons were responsive to multiple kinds of image statistics.
- Responses to 1- and 2-point statistics were common (~50%) in V1 and V2.
- Responses to 3- and 4-point statistics were rare (~10%) in V1 but more common (~20%) in V2, especially in the supragranular layers, confirming Yu et al., (2015).
- Responses were opponent-like, often with biases for either positive or negative values of the image statistic.
- The population has a bias towards darks (γ<0) in both V1 and V2 (Yeh et al., 2009, Kremkow et al., 2014).</li>

### Combinations of image statistics (the planes):

- Typical neurons had largest responses to mixtures of image statistics.
- Interactions of image statistics varied widely across neurons.
  Rare neurons responded in a non-monotonic fashion to variation in image statistics, suggesting that they participate in a distributed representation of the perceptual space.

#### References

- Conte, M.M., Rizvi, S.M., and Victor, J.D. (2015) Approximately uniform isodiscrimination contours within a perceptual space of local image statistics. Vision Sciences Society Annual Meeting, St. Petersburg, FL, 2015.

  Hermundstad, A. M., Briguglio, J.J., Conte, M.M., Victor, J.D., & Balasubramanian, V. (2014) Variance predicts salience in
- central sensory processing. eLife 3, doi:10.7554/eLife.03722.

  Kremkow, J., Jin, J., Komban, S.J., Wang, Y., Lashgari, R., L X., Jansen, M., Zaidi, Q., Alonso, J.M. (2014) Neuronal nonlinearity explains greater visual spatial resolution for darks than lights. Proc Natl Acad Sci USA 111, 3170-3175
- darks than lights. Proc Natl Acad Sci USA 111, 3170-3175
  Rizvi, S.M., Conte, M.M. & Victor, J.D. (2014) Border salience
  reveals a curved global geometry of the perceptual space
  of local image statistics. Vision Sciences Society Annual
  Meeting, St. Petersburg, FL, 2014.
  Tkačik, G., Prentice, J. S., Victor, J. D. & Balasubramanian, V.
- (2010) Local statistics in natural scenes predict the salience of synthetic textures. Proc Natl Acad Sci USA 107, 18149-18154.
- Victor, J. D. & Conte, M. M. (2012) Local image statistics: maximum-entropy constructions and perceptual salience. J Opt Soc Am A Opt Image Sci Vis 29, 1313-1345.

  Victor, J. D., Thengone, D. J. & Conte, M. M. (2013) Perception
- of second- and third-order orientation signals and their interactions. J Vis 13, 21, doi:10.1167/13.4.21.

  Yeh, C. I., Xing, D. & Shapley, R. M. (2009) "Black" responses dominate macaque primary visual cortex v1. J Neurosci 29,
- 11753-11760.

  Yu, Y., Schmid, A. M. & Victor, J. D. (2015) Visual processing of informative multipoint correlations arises primarily in V2.

eLife 4, doi:10.7554/eLife.06604.

Support: NIH EY9314